Materials Research Proceedings **26** (2023) 133-138 https://doi.org/10.21741/9781644902431-22

Tensile behaviour of rayon cords in different conditions

Lucas Pires da Costa[1,a], Giorgio Novati[1,b], Paola Caracino[2,d] , Claudia Comi[1,c], Simone Agresti[2,e]

[1]Department of Civil and Environmental Engineering, Politecnico di Milano, Italy

[2]R&D Reinforcement Materials – Pirelli Tyre SpA, Italy

[a]lucas.piresdacosta@polimi.it, [b]giorgio.novati@polimi.it, [c]claudia.comi@polimi.it, [d]paola.caracino@pirelli.com, [e]simone.agresti@pirelli.com

Keywords: Rayon Twisted Yarns, Tensile Tests, Elasto-Viscoplastic Behaviour

Abstract. Different polymeric fibrous materials, such as polyester, nylon, aramid and rayon, can be employed as reinforcement in tyres or in other rubber composites. The present contribution focuses on the experimental characterization of rayon yarns and cords and makes some steps towards developing a constitutive model for cords, to be later integrated into a finite element procedure for the analysis of fibre-reinforced composites. Uniaxial tensile tests under monotonic and cyclic loading together with creep tests have been performed on rayon specimens in different conditions. A simple, preliminary viscoelastic-viscoplastic model is proposed which can describe the main experimental findings for untwisted yarns.

Introduction

Cord-reinforced rubber components, such as tyres, are complex systems and the development of cost-effective computational methods for their analysis and for efficient product development at industrial level is still a challenging goal, see e.g. [1,2,3]. The knowledge of the material properties of the individual constituents and the ability to numerically simulate their behaviour represent important intermediate objectives. For cords, such task is rather demanding in view of the nonlinear constitutive behaviour of the fibres combined with the geometrical nonlinearities linked to the twisted structure of the material. This work reports on research activities conducted on rayon cords within an industry-academia collaboration in which the authors are involved. An extensive experimental campaign has been conducted and the obtained results, which highlight an elastic-viscoplastic behaviour of the cords, are discussed. Attention is given to the irreversible aspect of such behaviour, related to the manifestation of inelastic permanent deformations, which is rarely taken into consideration in the literature concerning polymeric fibres (while it is more often considered in the case of polymer matrix materials, see e.g. [4]). A rheological model is also proposed for the simulation of the behaviour of untwisted yarns.

Experimental tests on rayon yarns and cords

Representative results of the experimental campaign carried out by the authors on the materials in point are reported in [5]. For this reason and also due to space limitations, only a selection of the obtained experimental results, complementary to those described in [5], are reported in the present work; in particular some creep tests that were carried out only recently are here discussed.

Materials. All tested materials were either rayon filament yarns or cords made from them. The single untwisted yarn, denoted by Y0, has a linear density of 1840 dtex (g/10000 m) and contains 1000 filaments. Using two different twist levels applied to the same filament bundle, yarns Y38 and Y48 are obtained, with 380 and 480 turns per meter (tpm), respectively. Two cords (also called multi-ply yarns) are considered: cord C2, produced by twisting two Y48 yarns together; and cord C3, obtained by twisting three Y38 yarns together. For both cords, the twist direction of the filaments in the single yarn and the ply twist direction are opposite, with the same tpm value. Note

Materials Research Proceedings **26** (2023) 133-138 https://doi.org/10.21741/9781644902431-22

that only experimental results on greige materials are reported in the present work; some results for dipped cord can be found in [5].

Monotonic and non-monotonic tensile tests. A Zick-Roell testing machine with a 10 kN load cell was used to carry out the tests under displacement control, using different strain rates. The specimens were 500 mm long; bollard grips, suitable for filamentary materials, were employed. With reference to monotonic tests, we start showing some results that illustrate the influence of humidity conditions, see Fig. 1, and of strain rate, see Fig. 2. Note that "dry" conditions refer to samples that before being tested are kept in an oven at 100°C for at least two hours, while "humid" conditions apply to samples conditioned for 24 hours in the same climatic room where the test is run, at 20°C and at 65% of relative humidity. Each curve in Fig. 1 represents the mean response for ten experiments on nominally identical specimens. The adopted strain rate was 0.017 s^{-1}. It is apparent that rayon fibrous materials are very sensitive to moisture content: in dry conditions, the materials turn out to be generally stiffer and characterized by a higher maximum force and a lower maximum elongation than when humid. Note that yarn Y0 exhibits an almost bi-linear force-strain curve, interpretable as linear elastic in the first part and plastic with linear hardening in the second part. Figure 2 shows how the response of cords C2 and C3, in humid conditions, is affected by the adoption of different strain rates. Analogous experimental results for yarn Y0 are presented in Fig. 6 (b). As expected, both for the yarn and for the cords, the strength increases with the strain rate; the effect however is fairly limited, at least for the range of strain rates considered.

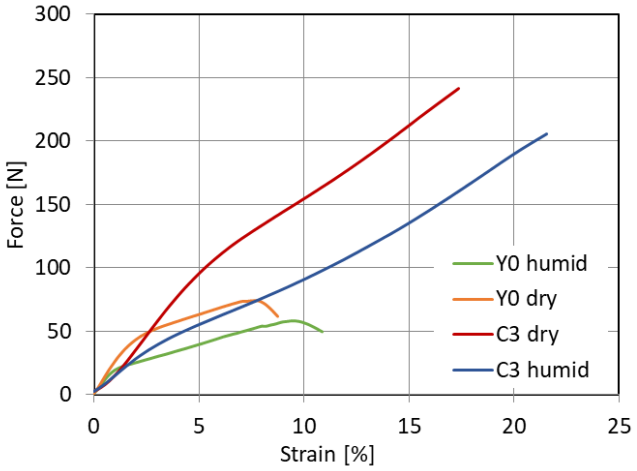

Fig. 1: Force-strain curves of uniaxial tensile tests in dry and humid conditions, for yarn Y0 and cord C3.

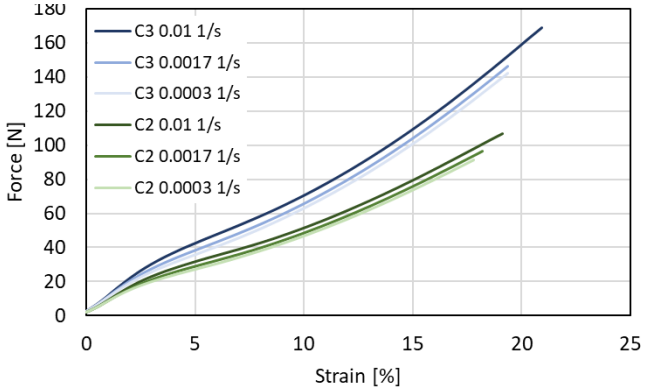

Fig. 2: Force-strain curves for monotonic tensile tests on cords C2 and C3.

Cyclic tests give important information on the inelastic behaviour of the materials under study. Such tests were performed under displacement control and using a constant strain rate ($\pm$ 0.003 s^{-1}), enforcing non-monotonic strain histories. Figure 3 shows the cyclic response of cords C2 and C3, under two different strain histories (in humid conditions). The two curves are plotted considering the average reactive force obtained from four tests on nominally identical samples. For cord C3, the same figure also depics the curve obtained imposing an increasing strain (linear in time), using the same strain rate of the cyclic tests. One can note the presence of permanent deformation upon unloading and of hysteresis loops in the unloading-reloading phases. An analogous behaviour is observed for yarn Y0, see Fig. 7 (a). The above results indicate an elastic-viscoplastic behaviour of rayon fibres and cords.

Creep tests. Very recently the experimental campaign has been enriched with some creep tests that give important additional information on the time-dependent properties of the materials under

Materials Research Proceedings **26** (2023) 133-138 https://doi.org/10.21741/9781644902431-22

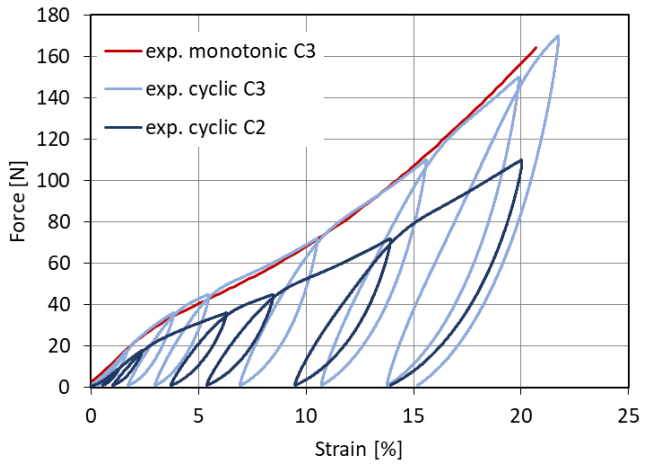

Fig. 3: Force-strain curves for cord C3 (cyclic and monotonic case) and for cord C2 (cyclic case only).

study. In all the creep tests, 200 mm long samples are used. Each test is carried out on two or three specimens and the reported result is the average obtained from the different specimens.

Figure 4 (a) shows the strain response to a creep test conducted on yarns Y0 and Y48 under a constant force of 10 N, holding this force for 24h (86400 s); the experiments are carried out at 20°C and at 65% of relative humidity. The tests were done by imposing increasing values of strain, for $0 < t < t_0$, up to the attainment of the given force; thereafter the force is kept constant. The strain at time t_0, denoted by ε_0, is called instantaneous strain. For the yarns Y0 and Y48 such strains (indicated by dotted horizontal lines in the graphs) turn out to be $\varepsilon_0^{Y0} = 0.7\%$ and $\varepsilon_0^{Y48} = 1.7\%$; note that the imposed load is such that the instantaneous response can be considered elastic. For both yarns, creep strain develops with an ever-decreasing strain rate. Denoting by ε_f^{Y0} and $\varepsilon_f^{Y48}$the final strains at the end of the experiment (i.e. after 24 h), the values obtained are $\varepsilon_f^{Y0} = 1.8\%$ and $\varepsilon_f^{Y48} = 4.5\%$; thus the ratios $\varepsilon_f^{Y0}/\varepsilon_0^{Y0} = 2.57$ and $\varepsilon_f^{Y48}/\varepsilon_0^{Y48} = 2.65$ turn out to be similar.

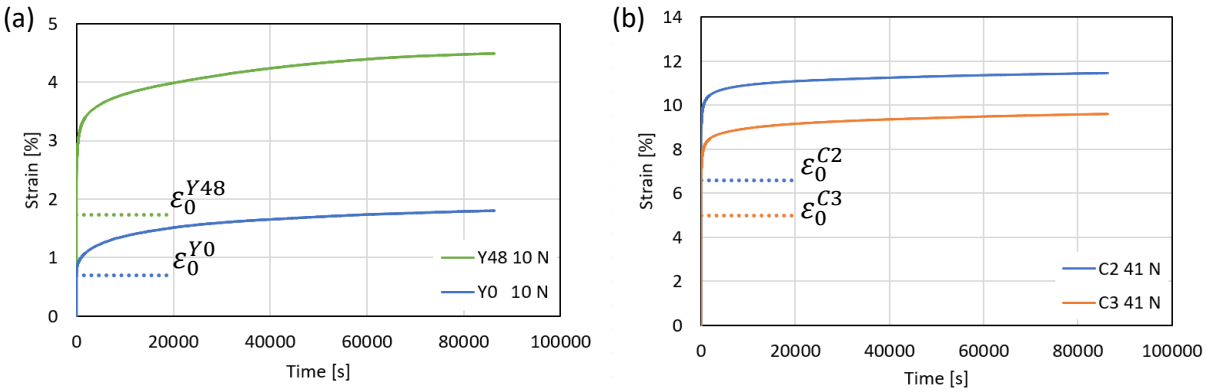

Fig. 4: Creep tests (a) for two yarns (Y0, Y48) and (b) for two cords (C2, C3) under different loads; the horizontal dotted lines mark the values of the so-called instantaneous strains.

Analogous results for creep test carried out for cords C2 and C3 are reported in Fig. 4 (b). The two cords were loaded by a (constant) force of 41 N (identical for C2 and C3); for both cords this load level is higher than the elastic limit (determined by monotonic tensile tests). Therefore, the instantaneous strain (denoted by ε_0) comprises elastic and inelastic contributions; it turns out that $\varepsilon_0^{C2} = 6.6\%$ and $\varepsilon_0^{C3} = 5\%$.

We also carried out creep tests at 100°C using the thermal chamber of Fig. 5 (a); note that these tests include load removal and a recovery phase. The results for cord C2 are shown in Fig. 5 (b) for two values of applied force (26 N, 83 N), held constant for 12600 s (3.5 h). The same figure shows also the creep response of cord C2 at 20°C and in humid condition (test conducted without the thermal chamber), under a load of 41 N. In Fig. 5 (b), the values of the "instantaneous" strains are marked by dotted horizontal segments, similarly to in Fig. 4.

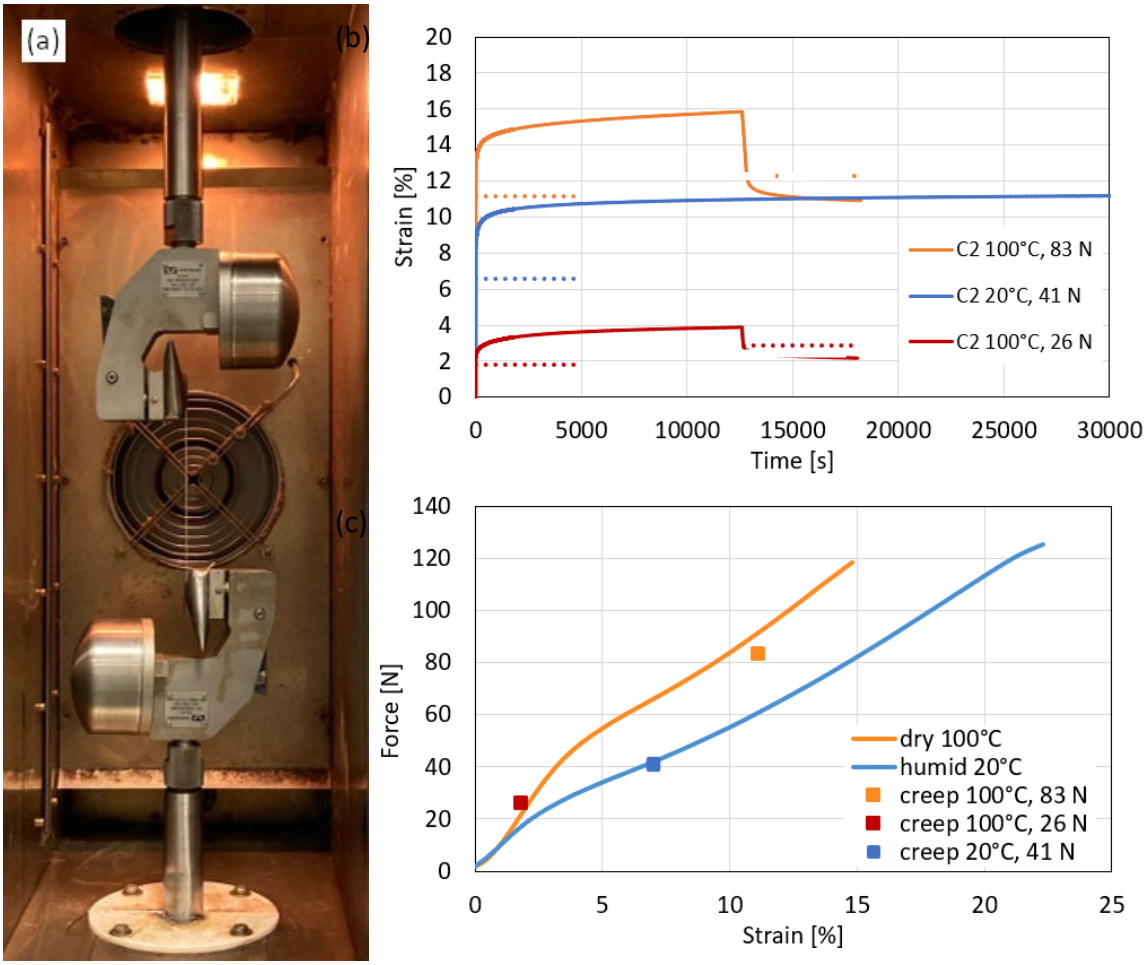

Fig. 5: (a) Thermal chamber for tests at high temperature; (b) creep-recovery response, at 100°C, for cord C2 and creep response for the same cord at 20°C (in humid conditions); (c) results from corresponding uniaxial tests on cord C2, performed at the same conditions.

Figure 5 (c) shows the result of the uniaxial tests on cord C2 performed at the same conditions employed in the creep tests. A square symbol is used to denote the force-strain values representing the "instantaneous response" at the beginning of the creep tests: in principle these square symbols should lie on the corresponding curves; the largest discrepancy can be noted for the creep instantaneous response at the higher load. One can note that among the three instantaneous strains shown in Fig. 5 (b-c), only the one corresponding to the lower load takes place in elastic regime.

Numerical simulation of the experimental behaviour of the untwisted yarn Y0

Viscoelastic-viscoplastic model. The one-dimensional rheological model depicted in Fig. 6 (a) consists of a linear spring (E) in series with a Kelvin unit ($\tilde{\boldsymbol{E}}, \tilde{\boldsymbol{\eta}}$) and with a viscoplastic unit comprising three elements in parallel: a frictional device ($\boldsymbol{\sigma_y}$), a hardening spring (H) and a viscous dashpot ($\boldsymbol{\eta}$). All elastic and viscous parameters are meant to be constant.

The total strain is hence the sum of three contributions: elastic, viscoelastic and viscoplastic:

$$\varepsilon = \varepsilon^{e} + \varepsilon^{ve} + \varepsilon^{vp} \tag{1}$$

Such 6-parameter model can represent the behaviour of a polymeric fibrous material, not accounting however for the geometric effects due to the twisted structure of yarns and cords; therefore, it is used only to simulate the behaviour of the untwisted yarn Y0.

Materials Research Proceedings **26** (2023) 133-138 https://doi.org/10.21741/9781644902431-22

By introducing a time discretization ($\Delta t = t_n - t_{n-1}$ denoting the time step) and assuming that (i) the state of the model is known at time t_{n-1} and that (ii) the strain ε_n at t_n is given (strain-driven process), it is possible to develop an integration algorithm over the time step for the updating of all the model variables to time t_n. The algorithm, based on Euler backward scheme, parallels the predictor/corrector scheme of classical rate-independent plasticity and makes use of "trial quantities" defined by "freezing" the viscoplastic strain ε^{vp} in the step. Thus, for any give strain history $\varepsilon(t)$, the response of the 6-parameter model can be obtained by an incremental method in time, with no iterations within each increment.

Note that for the above model, the creep response under a suddenly applied load $\bar{\sigma}$ can be obtained analytically and reads:

$$\varepsilon(t) = \bar{\sigma}/E + \bar{\sigma}/\tilde{E}\left(1 - exp\left(-\tilde{E}t/\tilde{\eta}\right)\right) + (\bar{\sigma} - \sigma_y)(1 - exp(-Ht/\eta))/H \quad (2)$$

where the last term is present only for $\bar{\sigma} > \sigma_y$.

Comparison between experimental results and numerical simulations. The yarn Y0 experimental results in terms of force, for the monotonic and cyclic tests, have to be expressed in terms of stress in order to be compared with results obtained by the 6-parameter model using the same strain history. The force values are divided by a nominal cross-section area A of yarn Y0, setting A = 0.17 mm² according to a microscopic measurement reported in [5].

A parameter identification is conducted in order to obtain a best fit with the yarn Y0 experimental behaviour under different load conditions (monotonic, cyclic and creep), always at 20°C and 65% humidity. The chosen values for the model parameters are: E = 12 GPa, $\tilde{E}$ = 4.5 GPa, $\tilde{\eta} = 5 \cdot 10^4$ GPa·s, H = 3.2 GPa, η = 3.5 GPa·s, σ_y = 90 MPa. Figure 6 (b) shows the comparison between monotonic experimental results at different strain rates (continuous lines) and the numerical results obtained using the model (dotted lines). The latter is able to replicate the influence of different velocities, producing a reasonable agreement with the tests.

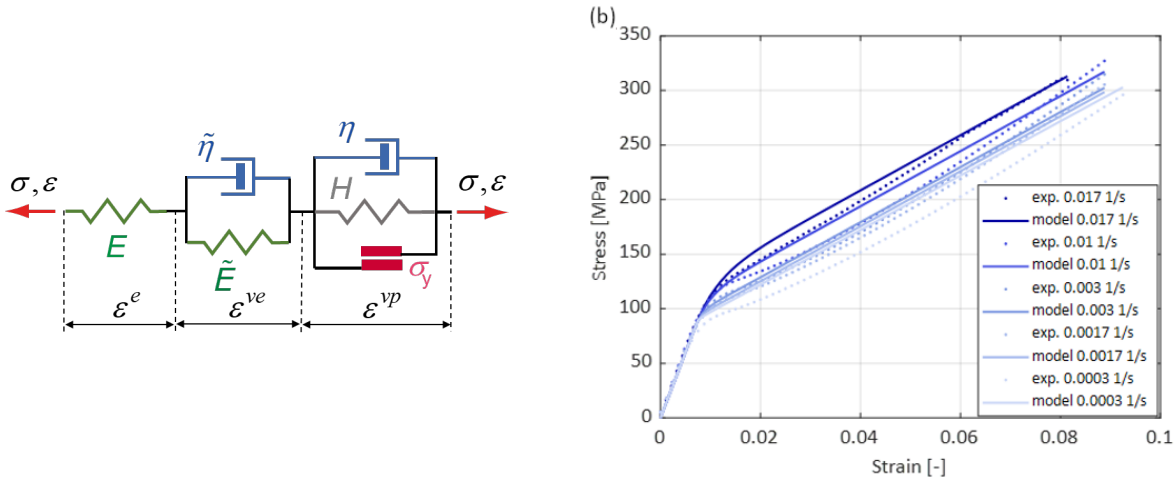

Fig. 6: (a) 6-parameter model; (b) comparison between experimental and numerical results for yarn Y0 under monotonic load at different strain rates (20°C, humid).

Figure 7 (a) compares the model and the experimental response to a given cyclic strain history (strain rate of 0.003 1/s) and shows fairly good agreement between the two curves. Figure 7 (b) shows the comparison between the creep test response in terms of strain and the model response based on Eq. 2, with the same set of parameters specified above.

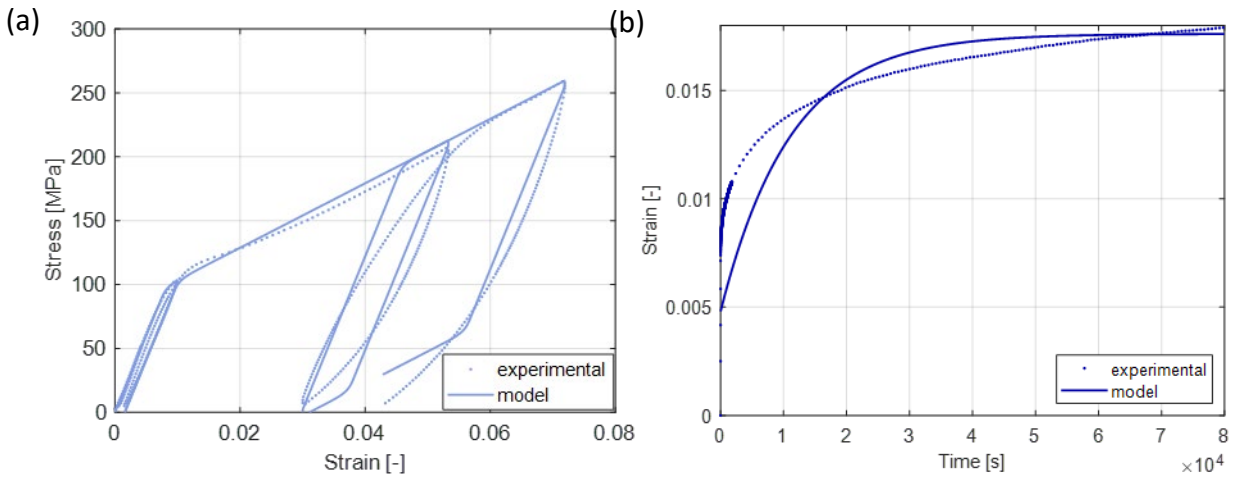

Fig. 7: Comparison between experimental data and results obtained with the 6-parameter model for yarn Y0 (at 20°C in humid conditions) for (a) cyclic load and (b) creep test.

Summary

In the present contribution, the elasto-viscoplastic behaviour of greige rayon yarns and cords was discussed on the basis of several experimental tests under monotonic and cyclic loading and under creep conditions. It was shown that the behaviour of untwisted rayon yarns can be fairly well represented by a 6-parameter viscoelastic-viscoplastic model. Current research is focusing on how to couple the fibre material behaviour and the geometrical effects due to the twisted structure of yarns and cords. With reference to such effects, it is worth noting that recent investigations using microtomography techniques [6] have led to a better understanding of fibre trajectories and of their evolution in twisted cords under tension.

References

[1] P. Helnwein, C. H. Liu, G. Meschke, H. A. Mang, A new 3-D finite element model for cord-reinforced rubber composites - application to analysis of automobile tires, Finite Elements in Analysis and Design 14 (1993) 1-16. https://doi.org/10.1016/0168-874X(93)90075-2

[2] M. G. Pastore Carbone, Investigating mechanical behavior of cord-rubber composites by multi-scale experimental and theoretical approach, PhD Thesis, Università degli Studi di Napoli Federico II, 2011.

[3] H. Donner, J. Ihlemann, On the efficient finite element modelling of cord-rubber composites, in: Constitutive Models for Rubber VIII – Proc. 8th European Conf. on Constitutive Models for Rubbers, ECCMR, 2013, pp. 149-155.

[4] R. K. Goldberg, G. D. Roberts, A. Gilat, Implementation of an associative flow rule including hydrostatic stress effects into the high strain rate deformation analysis of polymer matrix composites, J. of Aerosp. Eng., 18 (2005) 18-27. https://doi.org/10.1061/(ASCE)0893-1321(2005)18:1(18)

[5] P. Caracino, S. Agresti, L. Pires da Costa, G. Novati, C. Comi, The nonlinear behaviour of cords to be used in rayon-rubber composites, European Conference on Constitutive Models for Rubbers (ECCMR), Sept 7-9, 2022. https://doi.org/10.1201/9781003310266-77

[6] A. Sibellas, M. Rusinowicz, J. Adrien, D. Durville, E. Maire, The importance of a variable fibre packing density in modelling the tensile behaviour of single filament yarns, Journal of the Textile Institute, 112(5) (2021) 733-741. https://doi.org/10.1080/00405000.2020.1781347